Unveiling Residual Molecular Binding in Triply Charged Hydrogen Bromide

F. Penent,[1,2] P. Lablanquie,[1,2] J. Palaudoux,[1,2] L. Andric,[1,2,3] G. Gamblin,[1,2] Y. Hikosaka,[4] K. Ito,[5] and S. Carniato[1,2]

[1]*UPMC, Université Paris 06, LCPMR, 11 rue Pierre et Marie Curie, 75231 Paris Cedex 05, France*
[2]*CNRS, LCPMR (UMR 7614), 11 rue Pierre et Marie Curie, 75231 Paris Cedex 05, France*
[3]*Université Paris-Est, 5 boulevard Descartes, 77454 Marne-la-Vallée Cedex 2, France*
[4]*Department of Environmental Science, Niigata University, Niigata 950-2181, Japan*
[5]*Photon Factory, Institute of Materials Structure Science, Oho, Tsukuba 305-0801, Japan*

(Received 6 January 2011; published 11 March 2011)

We present an experimental and theoretical study of triply charged hydrogen bromide ions formed by photoionization of the inner 3*d* shell of Br. The experimental results, obtained by detecting the 3*d* photoelectron in coincidence with the two subsequent Auger electrons, are analyzed using calculated potential energy curves of HBr^{3+}. The competition between the short-range chemical binding potential and the Coulomb repulsion in the dissociative process is shown. Two different mechanisms are observed for double Auger decay: one, a direct process with simultaneous ejection of two Auger electrons to final HBr^{3+} ionic states and the other, a cascade process involving double Auger decay characterized by the autoionization of Br^{*+} ion subsequent to the HBr^{2+} fragmentation.

DOI: 10.1103/PhysRevLett.106.103002 PACS numbers: 32.80.Fb, 33.60.+q

While molecular dications have been the subject of many experimental and theoretical studies [1], little is known about molecular M^{3+} trications. In most cases, the Coulomb repulsion leads to their fast fragmentation. It is only recently that the associated dissociation dynamics, such as the complete atomization of SO_2^{3+} [2] or CO_2^{3+} [3,4], could be probed with Coulomb explosion imaging techniques. Although multiply charged ions from large molecules or clusters have been observed in mass spectroscopy, only a few small metastable triply charged molecular ions have been found, among which CS_2^{3+} is the best documented example [5]. Metastable dihalogen trications were also observed [6] and identified [7]. The first extensive calculation of M^{3+} dissociative states was undertaken in Cederbaum's group 15 years ago for CO^{3+} [8], followed by Brandauk *et al.* [9] for N_2^{3+}. They revealed the complexity of the problem due to many possible coupled final states.

In this Letter we demonstrate with the HBr^{3+} example that detailed knowledge of individual dissociative tricationic states can be obtained. Calculated HBr^{3+} potential curves have been probed experimentally through the double Auger (DA) process following Br 3*d* inner-shell ionization. The topology of these trication states, arising from chemical bonding effects is evidenced in the observation of the lower HBr^{3+} states and the HBr^{2+} Rydberg series converging to these limits.

Photoionization can be used to form HBr^{3+} trications through different pathways. Below the inner-shell ionization threshold, the valence triple photo-ionization (TPI) process is allowed, but, experimental studies of Argon [10] would suggest that the TPI process only occurs with a small probability. Once the inner-shell ionization channel opens, DA decay of HBr^+ $(3d^{-1})$ leads to substantial HBr^{3+} formation, as DA probability amounts to $\sim$10% of single Auger decay. This process can be compared to that of the isoelectronic Kr atom [11]. In both cases, the threshold for 3*d* inner-shell ionization lies about 20 eV above the TPI threshold so that DA decay is energetically allowed.

In Fig. 1, we present our calculated HBr^{3+} potential energy curves of the adiabatic states correlated to the $H^+ + Br^{2+}$ (^4S, ^2D, ^2P) dissociation limits. The spin-orbit splitting of the Br^{2+} $^2D_{5/2,3/2}$ and $^2P_{3/2,1/2}$ final states is neglected. The calculations use a method based on *ab initio* multireference multistate perturbation theory which allows for the inclusion of nondynamic and dynamic electronic correlations, up to the dissociation limit. The results reveal a peculiar topology arising from the dominating Coulomb repulsion in the (H^+, Br^{2+}) system combined with the short-range chemical binding of the (H, Br^{3+}) system. In the Franck-Condon (FC) region, the binding, while appreciable, is not strong enough to create a local potential minimum [5–7]. In Fig. 1 the energy crossing of the quartet state II (correlated to the $H^+ + Br^{2+}$ (^4S) limit) with the lowest doublet state I correlated to Br^{2+} (^2D) around $R = 1.8$ Å is observed. This implies that, in the FC region, the lowest HBr^{3+} state is a doublet state. The potential energy curves of the intermediate HBr^+ $(3d^{-1})$ states have also been calculated allowing the determination of FC factors between these states and HBr^{3+} final states.

Experiments were performed on the U56/2 PGM2 beam line [12] of the BESSY-II synchrotron during single bunch operation that gives a $T = 800.5$ ns light pulse period. The electron spectrometer is a long ($\sim$ 210 cm) magnetic bottle time-of-flight spectrometer that has been described in detail previously [11,13]. Its collection efficiency is over

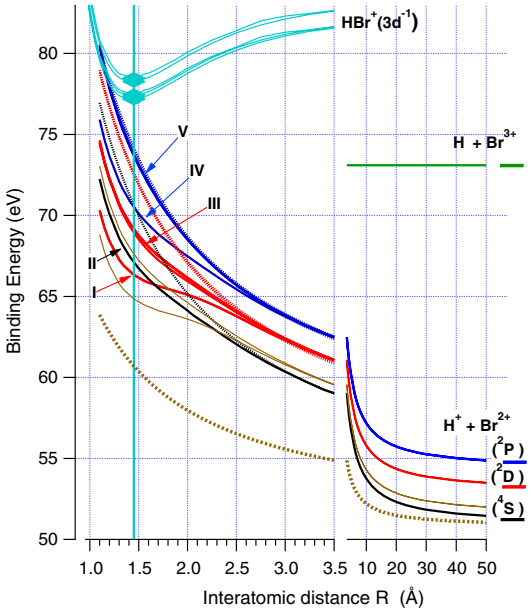

FIG. 1 (color online). Calculated potential curves of HBr^+ $(3d^{-1})$ (light blue) and of HBr^{3+} states correlated to $H^+ + Br^{2+}(^4S)$ (black), (^2D) (red) and (^2P) (blue) (note the change in R scale at $R = 3.5$ Å). The dot curves represent the $(+1)(+2)/R$ Coulomb potential starting from the $H^+ + Br^{2+}$ limits. The thin (brown) lines correspond to HBr^{2+} $n = 6$ Rydberg states bound to the (red) curves. The thick dashed (brown) curve represents the $1/R$ Coulomb potential between H^+ and Br^+. The vertical line indicates FC zone associated to the HBr equilibrium distance.

95% of the full solid angle and the detection efficiency is ~55% for electrons between 0 to 200 eV as was determined experimentally using coincident detection of Kr $(3d)$ photoelectrons with Auger electrons. A mechanical chopper [14] was used to increase this period to a mean value of 12.5 μs allowing the determination of the absolute electron time of flight (TOF). The TOF of the successive electrons are measured by a time-to-digital converter (250 ps time resolution) with respect to the ring clock signal gated by the detection of the photon bunch going through the chopper using a channeltron inserted in the beam at the end of the chamber. The time-to-energy conversion and calibration uses He photoelectrons at different photon energies and known Auger transitions in rare gases. The photoelectron energy was chosen around 25 eV so that the $3d$ photoelectron is faster than the two Auger electrons from DA decay detected in coincidence with it. At 25 eV, the energy resolution $\Delta E/E = 1.6\%$ is enough to resolve the 1.25 eV spin orbit splitting of the $3d_{3/2}$ and $3d_{5/2}$ levels but not the molecular field splitting [15]. All data presented here correspond to the detection of three electrons in coincidence by selecting the corresponding events in the data list. The electron count rate was limited in the 1–3 kHz range to keep the contribution of random coincidences negligible.

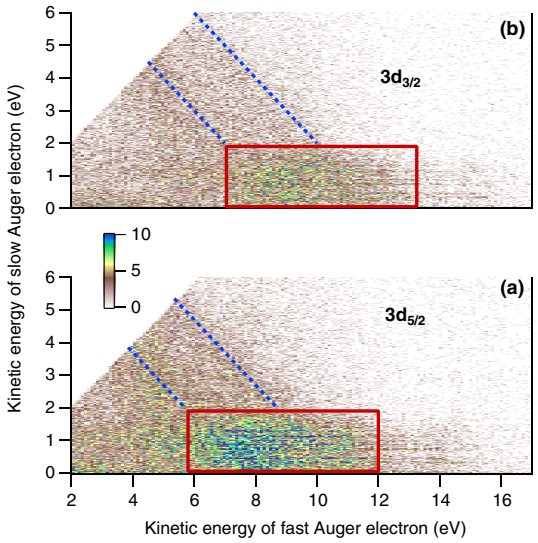

FIG. 2 (color online). 2D coincidence map between two Auger electrons detected in coincidence with a $3d_{5/2}$ (a) or a $3d_{3/2}$ (b) photoelectron. Dashed (blue) diagonal lines indicate direct double Auger decays populating HBr^{3+} states in the FC zone. Rectangles (red) correspond to the prominent two-step process.

Figure 2 displays the energy correlation map between the two Auger electrons emitted in the DA decay of a Br $3d_{3/2}$ or $3d_{5/2}$ vacancy. The spectra appear blurred compared to the Kr atomic case [11], because the final HBr^{3+} states are repulsive molecular states with a large dE/dR slope in the Franck-Condon region. Figures 2(a) and 2(b) are very similar and appear to be simply shifted in energy along the x axis, by the $3d$ spin orbit splitting of 1.25 eV. Two different zones of interest can be identified in these 2D maps. The highest intensity is observed for $0 < E_{A2} < 2$ eV and $6 < E_{A1} < 12$ eV and is characterized by horizontal lines. The specific two-step process associated with this region will be described later. We will concentrate first on the diagonal structures that are visible for $E_{A2} > 2$ eV and $6 < E_{A2} + E_{A1} < 12$ eV. In Fig. 3 the projection of the 2D spectra on the $x = y$ axis is shown for $E_{A2} > 2$ eV; it corresponds to the histogram of $E_{A1} + E_{A2}$. It is directly converted into binding energy E_B of the final HBr^{3+} states by

$$E_B(HBr^{3+}) = E_B[HBr^+(3d^{-1})] - (E_{A2} + E_{A1}) \quad (1)$$

The energy distribution along the diagonal $E_{A1} + E_{A2} =$ constant, indicates a continuous energy sharing between the two Auger electrons compatible with a direct double Auger decay towards HBr^{3+} final states. Because of the strong $2/R$ Coulomb repulsion between H^+ and Br^{2+} the dynamics of Coulomb explosion of HBr^{3+} into $H^+ + Br^{2+}$ might compete with double Auger decay in the femtosecond time scale.

Figure 3 displays the population of HBr^{3+} states populated in $3d$ direct DA decay: $3d_{5/2}$ and $3d_{3/2}$ decays give similar results. The contribution of each HBr^{3+} state is

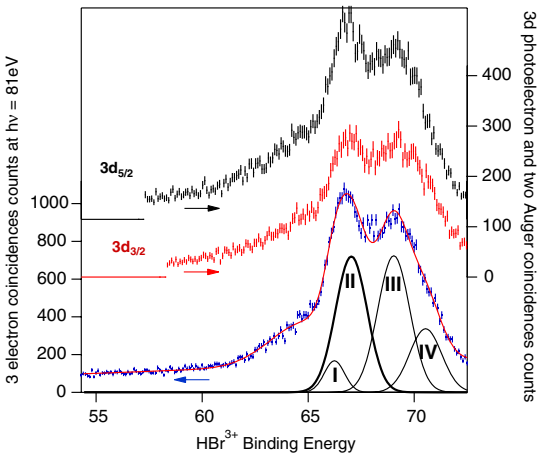

FIG. 3 (color online). HBr^{3+} states populated in a direct DA decay. The (black and red) data curves were obtained at a photon energy of 105 eV and correspond to the histograms of $E_{A1} + E_{A2}$ from Figs. 2(a) and 2(b) when $E_{A2} > 2$ eV. An offset is used for the $3d_{5/2}$ black curve. The (blue) data were obtained at a photon energy of $h\nu = 81$ eV from all three electron coincidences with energies $E_i > 2$ eV. E_B is then deduced from $E_B = h\nu - (E_1 + E_2 + E_3)$. The (blue) data are fitted using calculated FC profiles revealing individual HBr^{3+} final states (see text).

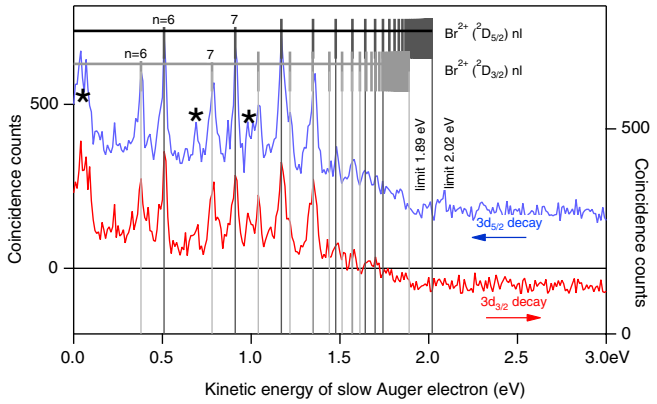

FIG. 4 (color online). Projection of the 2D spectra from Fig. 2 on the y axis with identification of two Br^{+*} Rydberg series built on Br^{2+} $^2D_{3/2}$ and $^2D_{5/2}$ cores.

retrieved by using our calculated FC profiles. The fit in Fig. 3 was obtained by adjusting only the relative amplitude of the different final states while keeping fixed the energies at their calculated theoretical value. Because of the broad (~ 2 eV) FC distributions resulting from the repulsive potential it is not necessary to consider the spin-orbit splitting of the $^2D_{3/2,5/2}$ (~ 130 meV) and $^2P_{1/2,3/2}$ (~ 200 meV) Br^{2+} states. The agreement with experiment is excellent by considering only the four lower molecular curves shown in Fig. 1 with a prominent decay to curves II (quartet state) and III (unresolved doublet states). It clearly reveals the residual chemical binding of HBr^{3+} in the FC region with respect to the repulsive $2/R$ Coulomb potential (~ 6.3 eV for ground state I and ~ 3.5 eV for states II, III, and IV). Such agreement is a strong indication that, in the region of interest in the 2D map in Fig. 2, direct double Auger decay precedes the Coulomb explosion of the HBr^{3+} ion and that the hypothesis of fixed nuclei during double Auger decay holds. A small bump structure below 65 eV binding energy in Fig. 2 is not matched by the calculated FC factors. It might be associated with a two-step Auger decay. Firstly, a first Auger electron is emitted to a HBr^{2+} state (Rydberg states converging to HBr^{3+} limit). Subsequently, this ion dissociates and a second electron can be emitted in the molecular region once the HBr^{2+} dissociative curve goes above the HBr^{3+} curve. In such case, two electrons can transport more energy than what is allowed for direct DA decay with fixed nuclei.

This kind of process is confirmed in the strongest Auger decay process observed in Fig. 2 [(red) rectangles]. The projection of the 2D map on the y (E_{A2}) slow energy axis is given in Fig. 4. The projection is similar for the $3d_{5/2}$ and $3d_{3/2}$ initial core hole and shows many discrete energy peaks. Such peaks reveal atomic autoionization. The only decay channel able to produce discrete energy electrons in HBr TPI is autoionization of a Br^+ ion after fragmentation of the HBr^{2+} state produced by Auger decay:

$$\begin{aligned} \mathrm{HBr} + h\nu &\rightarrow \mathrm{HBr}^+(3d^{-1}) + e_{\mathrm{ph}} \\ &\rightarrow \mathrm{HBr}^{2+} + e_{A1} \\ &\rightarrow \mathrm{H}^+ + \mathrm{Br}^{+*} \\ &\rightarrow \mathrm{Br}^{2+} + e_{A2}. \end{aligned} \tag{2}$$

This process is demonstrated by the assignment of most of the observed atomic peaks in two Rydberg series (with zero quantum defect) converging to 1.89 and 2.02 eV, separated by 0.130 eV. The 2.02 eV limit corresponds to the energy of the $^2D_{5/2}$ Br^{2+} level relative to the ^4S state according to NIST reference tables, but the reported $^2D_{3/2}$-$^2D_{5/2}$ energy splitting is given at 0.156 eV [16]. An anomaly was first noticed by Person *et al.* [17] for the ^2D splitting of Br III in its isoelectronic sequence. A new interpretation on the Br III spectra [18] positions the $^2D_{3/2}$ at 1.89 eV and the $^2D_{5/2}$ at 2.021 eV above the Br^{2+} ^4S ground state and reveals errors in the original data interpretation [16,19] that was kept in databases [16].

We confirm here the 130 meV spin-orbit splitting of the $^2D_{5/2,3/2}$ Br^{2+} states. The observed Rydberg series are $Br^{2+}(^2D_{5/2})nl$ and $Br^{2+}(^2D_{3/2})nl$ series (with $n = 6$ to 12) that autoionize to Br^{2+} ^4S ground state. The observed peaks show that autoionization occurs after fragmentation of HBr^{2+} at an internuclear distance large enough to neglect molecular effects. A few peaks [asterisks in Fig. 4] are not assigned. The prominent peak at 0.1 eV could possibly be a $Br^{2+}(^2D_{3/2})5l$ state with a small quantum defect.

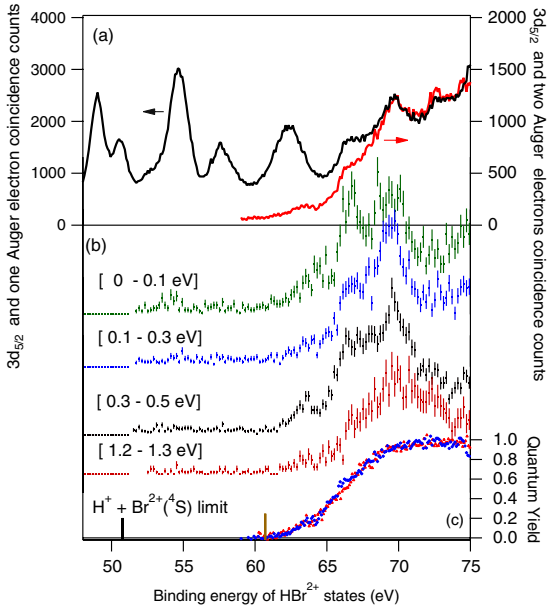

FIG. 5 (color online). (a) Black line: HBr^{2+} states populated by single Auger decay of the $3d_{5/2}$ hole, and located above the $H^+ + Br^{2+}(^4S)$ limit at 50.77 eV. Grey (red) line: HBr^{2+} states evolving in a double Auger decay. (b) HBr^{2+} intermediate states involved in the production of selected autoionizing Br^{+*} states in reaction (2). (c) HBr^{2+} autoionization quantum yield, deduced from the ratio of the curves in (a). Dark (blue) and light (red) points are obtained, respectively, from the $3d_{5/2}$ and $3d_{3/2}$ decays.

We consider now the identification of the HBr^{2+} precursor states in reaction (2). They are extracted in Fig. 5(b) from the energy distribution of the first Auger electron associated with the atomic autoionization electrons. Some structures are visible that are compatible with molecular Rydberg states such as those indicated in thin (brown) line in Fig. 1. The lower energy structure at about 64 eV [Fig. 5(b) (0.3–0.5 eV)] can be assigned to a $n = 6$ HBr^{2+*} Rydberg state whose core is the ground HBr^{3+} doublet state. Figure 5(a) displays the higher excited HBr^{2+*} states populated by single Auger decay, as deduced from the $3d_{5/2}$ coincident Auger spectrum. These states can eventually further decay by emission of a second Auger electron, as represented by the (red) curve deduced from three electron coincidences ($3d_{5/2}$ photoelectron and two Auger).

Taking into account the experimental detection efficiency, the ratio of the (red and black) curves from Fig. 5(a) gives in (c) the HBr^{3+} "quantum yield," as defined by Eland [1]. It represents the autoionization probability of these HBr^{2+*} excited states. The ~62 eV threshold is in good agreement with a $1/R$ repulsive potential correlated to $H^+ + Br^{2+}(^4S)$ limit [thick dashed (brown) curve in Fig. 1]. This supports the existence of dissociative HBr^{2+} states that can release a second electron during dissociation if they lie above the $H^+ + Br^{2+}(^4S)$ limit. The simple model puts this limit at 61 eV.

The study of double Auger decay by detection of three electrons in coincidence has revealed different decay processes. Direct double Auger decay has been observed and can be interpreted thanks to the calculation of HBr^{3+} molecular potential curves. A sequential decay process involving dissociation of HBr^{2+} Rydberg states provides spectroscopic data on Br^{+*} autoionizing Rydberg series. This study shows that even without the existence of any stable triply charged HBr^{3+} ions electron coincidence electron spectroscopy gives precise information on HBr^{3+} potential energy curves and reveals the remaining binding energy in the FC region.

This work was supported by the European Community Research Infrastructure Action under the FP6 "Structuring the European Research Area" Programme through the Integrated Infrastructure Initiative "Integrating Activity on Synchroton and Free Electron Laser Science," Contract No. R II 3-CT-2004-506008. We warmly acknowledge the support by the beam line scientists (B. Zada and W. Mahler) at BESSY.

[1] J. H. D. Eland, Adv. Chem. Phys. **141**, 103 (2009), and references therein.
[2] M. Lavollée and V. Brehms, J. Chem. Phys. **110**, 918 (1999).
[3] K. Ueda and J. H. D. Eland, J. Phys. B **38**, S839 (2005).
[4] N. Neumann *et al.*, Phys. Rev. Lett. **104**, 103201 (2010).
[5] J. H. D. Eland *et al.*, J. Chem. Phys. **132**, 104311 (2010).
[6] H. Sakai *et al.*, Phys. Rev. Lett. **81**, 2217 (1998).
[7] J. S. Wright *et al.*, Phys. Rev. A **59**, 4512 (1999).
[8] G. Handke, F. Tarantelli, and L. S. Cederbaum, Phys. Rev. Lett. **76**, 896 (1996); J. Chem. Phys. **104**, 9531 (1996).
[9] A. D. Bandrauk, D. G. Musaev, K. Morokuma, Phys. Rev. A **59**, 4309 (1999).
[10] Y. Hikosaka *et al.*, Phys. Rev. Lett. **102**, 013002 (2009).
[11] J. Palaudoux *et al.*, Phys. Rev. A **82**, 043419 (2010).
[12] K. J. S. Sawhney *et al.*, Nucl. Instrum. Methods Phys. Res., Sect. A **390**, 395 (1997).
[13] F. Penent *et al.*, Phys. Rev. Lett. **95**, 083002 (2005).
[14] K. Ito *et al.*, Rev. Sci. Instrum. **80**, 123101 (2009).
[15] T. Matila *et al.*, J. Phys. B **35**, 4607 (2002).
[16] Yu. Ralchenko *et al.*, (2010) NIST Atomic Spectra Database (ver.4.0.1) http://physics.nist.gov/asd [2010]; K. R. Rao and S. G. Krishnamurty, Proc. R. Soc. A **161**, 38(1937);
[17] W. Persson and S. G. Pettersson, Phys. Scr. **29**, 308 (1984).
[18] Y. N. Joshi *et al.*, Phys. Lett. A **113**, 479 (1986).
[19] Y. B. Rao, Indian J. Phys. B **35**, 386 (1961).